



HAL
open science

High-Field Solid-State NMR with Dynamic Nuclear Polarization

Daniel Lee, Sabine Hediger, Gaël De Paëpe

► **To cite this version:**

Daniel Lee, Sabine Hediger, Gaël De Paëpe. High-Field Solid-State NMR with Dynamic Nuclear Polarization. Modern Magnetic Resonance 2017, Springer International Publishing, pp.1-17, 2017, 10.1007/978-3-319-28275-6_73-1 . hal-02043260

HAL Id: hal-02043260

<https://hal.science/hal-02043260>

Submitted on 28 Sep 2021

HAL is a multi-disciplinary open access archive for the deposit and dissemination of scientific research documents, whether they are published or not. The documents may come from teaching and research institutions in France or abroad, or from public or private research centers.

L'archive ouverte pluridisciplinaire **HAL**, est destinée au dépôt et à la diffusion de documents scientifiques de niveau recherche, publiés ou non, émanant des établissements d'enseignement et de recherche français ou étrangers, des laboratoires publics ou privés.

High-Field Solid-State NMR with Dynamic Nuclear Polarization

Daniel Lee¹, Sabine Hediger^{1,2}, and Gaël De Paëpe¹

¹*Univ. Grenoble Alpes, INAC, F-38000 Grenoble, France and CEA, INAC, F-38000 Grenoble, France; and* ²*CNRS, INAC, F-38000 Grenoble, France.*

Keywords

Dynamic nuclear polarization, solid-state NMR, magnetic field, hyperpolarization, magic angle spinning, signal enhancement, polarizing agents, absolute sensitivity, microwave, biomolecules, materials.

Abstract – 250 words

Microwave induced dynamic nuclear polarization (DNP) can produce hyperpolarization of nuclear spins, leading to significant signal enhancement in NMR. This chapter discusses the contemporary application of DNP for solid-state NMR spectroscopy at high magnetic fields. The main mechanisms and polarizing agents that enable this hyperpolarization are presented, along with more practical aspects such as

the effect of decreasing sample temperature and analysing the absolute sensitivity gain from these experiments. Examples of the exploitation of DNP for studies of biomolecules, biominerals, pharmaceuticals, self-assembled organic nanostructures, and mesoporous materials are given as is an outlook as to the future this powerful technique.

Introduction

There has been a recent quasi-reinvention of dynamic nuclear polarization (DNP), in particular for use with solid-state (ss)NMR, even though its discovery was more than 60 years ago [1, 2]. The desire for high-resolution ssNMR, necessitating the use of large magnetic fields, hindered the large-scale development of ssNMR with DNP, although not completely [3], owing to practical technological constraints. These limitations were proved to be surmountable through the pioneering work of Griffin and co-workers, who showed that the use of low sample temperatures and cyclotron resonance masers (gyrotrons) as microwave sources could be combined with magic angle spinning (MAS) and high magnetic fields (≥ 5 T) to successfully and significantly increase the sensitivity of high-resolution ssNMR experiments through DNP (see Figure 1) [4]. This DNP effect, whereby the larger intrinsic polarization of electron spins is transferred to surrounding nuclear spins, has thereafter become an increasingly prominent part of modern ssNMR.

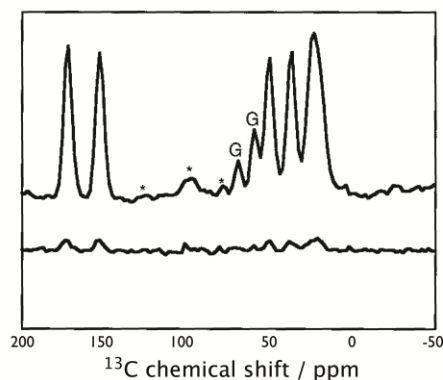


Fig. 1. $\{^1\text{H}\}\text{-}^{13}\text{C}$ CPMAS spectra of a frozen solution of $\text{U-}^{13}\text{C-}^{15}\text{N}$ -L-arginine (30 mg/ml in 60:40 water-glycerol with 40 mM 4-amino-TEMPO) recorded in a magnetic field of 5 T, at a sample temperature of 55 K, and with a MAS frequency of 3 kHz, with (top) and without (bottom) microwave irradiation. The peaks labeled with an asterisk correspond to rotational sidebands and those labeled G to glycerol peaks. Adapted from Ref. [4]. Reprinted with permission from AAAS.

Basic Theory and Methodology

There are many ways to achieve a polarization transfer between electron spins and nuclear spins, and the theory of the key contemporary mechanisms has been comprehensively discussed [5]. For the case of MAS-DNP, the theory is being constantly updated. In particular, an Overhauser effect (OE) has been observed for insulating solids [6], a scenario previously deemed not possible, and also the specific function of the MAS for cross-effect (CE) [7, 8] and solid-effect (SE) [7] DNP has also been detailed. Simply, the OE originates from the presence of a cross-relaxation process, zero (ZQ) or double quantum (DQ), resulting from a fluctuating hyperfine coupling (between an electron and a nuclear spin). When the difference between ZQ and DQ cross-relaxation rates is sufficient (and allows an efficient redistribution of populations), the microwave (μw) induced saturation of the electron Zeeman transition results in an enhancement of the nuclear polarization. Therefore, the OE relies on the relative relaxation rates in the system. Contrastingly the SE, which also involves a

coupling between an unpaired electron and a nuclear spin, is driven by a single-quantum (SQ) relaxation process and the ability to saturate a resolved “forbidden” ZQ or DQ transition, in order to enhance the nuclear polarization. Therefore, the SE relies on the applied μw power and the spin relaxation rates. The CE, however, requires the presence of three coupled spins (two electrons and one nucleus). The corresponding mechanism is significantly different under static and sample spinning conditions. With MAS, the (fixed-frequency) μw irradiation is used to periodically perturb the polarization of one electron spin (at a time) and generate a large electron polarization difference (compared to the nuclear Boltzmann polarization). The difference in polarization between the two coupled electrons can be transferred to the surrounding nuclei when the CE condition is fulfilled: when the difference in electron resonance frequencies matches the Larmor frequency of the nucleus. Such a MAS-DNP effect does then not require the μw and CE conditions to occur simultaneously. The detailed description and understanding of MAS-DNP processes has been enabled due to efficient quantum calculations, which are continuously being improved and currently allow their implementation on large spin systems [9, 11]. At this point it is also important to note that in the absence of μw irradiation and under MAS, the periodic repetition of CE matching conditions can induce a perturbation of the nuclear polarization. In some cases this can lead to a reduction of the detectable nuclear polarization (compared to Boltzmann equilibrium), creating a *depolarized* nuclear spin state [9, 10].

The OE, SE, and CE all permit the nuclear spin system to evolve to an equilibrium (non-Boltzmann) polarization state. The characteristic time constant for the spin system to reach this equilibrium state via DNP (commonly labelled T_{B}) is then different to the nuclear spin-lattice relaxation time constant, T_1 . Subsequent to this hyperpolarization buildup, ssNMR experiments are performed in their usual manner (i.e., no radio

frequency pulse sequence modifications need to be made). In fact, for MAS NMR in combination with CE-DNP, the MAS can actually dramatically improve the hyperpolarization efficiency [10]. Owing to its (relatively) consistently high hyperpolarization efficiency and ease of implementation, the CE is the most commonly used mechanism for high-field MAS-DNP. There are alternative methods for DNP, however these are only currently practicable on static samples at low magnetic field [5].

To make high-field DNP both practicable and practical for solid-state NMR spectroscopy, it was necessary to combine certain technologies and also to make these commercially available. As stated above, the introduction of gyrotrons as high-power, high-frequency μw sources as well as cooling systems and NMR probes allowing low temperatures (i.e., reduced spin relaxation rates) for MAS was pivotal to the recent major advances of the technique. Nevertheless, there have been other methodological milestones, such as the introduction of bi-radicals as exogenous polarizing agents [12]. An example of their chemical structure is given in Figure 2, along with that of two other typical radicals for DNP. These two other radicals, 1,3-bisphenylene-2-phenylallyl (BDPA, Figure 2a) and OX063 (a trityl-based radical, Figure 2b), and their derivatives, are normally employed for DNP-enhanced ssNMR using the SE, although BDPA has also been shown to provide efficient OE under MAS [6]. Bi-radicals (Figure 2c) were developed to produce efficient CE DNP. Originally, mono-nitroxide radicals, such as TEMPOL, were used for CE DNP of ^1H nuclei; mono-nitroxides are one half of the molecule shown in Figure 2c. A high concentration of mono-nitroxides would equate to a significant average inter-electron dipolar coupling and thus permit CE DNP. However, such a high concentration (usually ~ 40 mM) introduces significant detrimental paramagnetic effects to the system too. So, the *coup de maître* was the use

of chemically tethered nitroxide moieties, which have large electron-electron dipolar couplings without the need for a high concentration of radical species. This then enabled large ssNMR sensitivity gains with DNP, where the polarization from the bi-nitroxide electron spins can be transferred via the CE to ^1H spins that have a significant homonuclear dipolar coupling, allowing efficient propagation of their hyperpolarization throughout the entire ^1H spin system via spin-diffusion (ρ -type mechanisms). The ^1H hyperpolarization can then be transferred to the nuclei of interest through standard ssNMR methods, such as cross-polarization (CP). In recent years, the groups labelled 'R' in Figure 2c have been varied to edit the CE DNP properties [13]. This is also true for the tethering linker ('L' in Figure 2c) that connects two (or more) nitroxide moieties [13]. The linker has also been chemically modified in certain instances to perform particular tasks, such as to interact with an analyte, whether through chemical grafting [14] or chemical affinity [15].

Exogenous radicals like those in Figure 2 are much more frequently used as polarizing agents compared to endogenous or intrinsic radicals because it is easier to chemically control the characteristics of their electron spins, such as concentration, g -tensor anisotropy, couplings, and relaxation properties, leading to more efficient DNP, and also because most NMR samples do not inherently contain unpaired electrons. Nevertheless, high-field ssNMR studies using endogenous DNP have been performed, both for biological systems [16], as well as for materials [17], containing intrinsic paramagnetic sites. The returned signal gains from DNP were significantly below what could be achieved with exogenous polarizing agents. However, for "directed" (locally selective) DNP, for studies where one does not want to / cannot modify the sample with the addition of solvents or polarizing agents, and/or with improved technology (such as

access to lower sample temperatures) there is a growing interest for DNP using endogenous radicals.

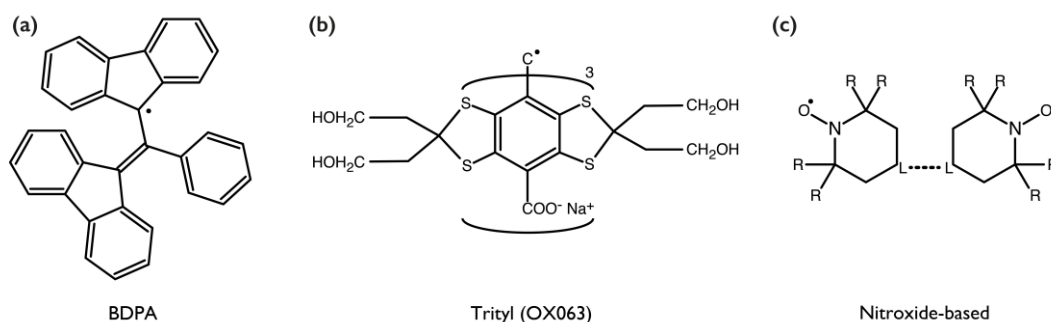


Fig. 2. Paramagnetic hyperpolarizing agents commonly used for high-field ssNMR with DNP: (a) 1,3-bisphenylene-2-phenylallyl (BDPA), (b) OX063, and (c) nitroxide. (c) can be mono-radical (without the linker, L) or multi-radical (with linker(s)). Both L and R moieties can be varied to modify the properties of the polarizing agent.

There is a current general limitation of minimum sample temperatures of ~ 100 K, which is related to the use of nitrogen gas to cool (and pneumatically spin, in the case of MAS) the sample. At a pressure of 2 bar, nitrogen liquefies at 85 K, imposing this limit on the sample temperature. Using cold helium gas instead of nitrogen would allow much lower sample temperatures (at 2 bar, helium liquefies at < 5 K) but this comes with technological difficulties and expense, especially when MAS is desired. Although high-field DNP-enhanced ssNMR experiments have been performed under static sample conditions with temperatures as low as ~ 4 K [18], most static experiments have been performed under the more conventional sample temperatures of ~ 100 K, with examples of biological (oriented membranes [19]), pharmaceutical (polymorphism of active ingredients [20]), and materials science (platinum-based catalysts [21]) applications. Obviously, certain circumstances dictate that MAS is not used during a ssNMR experiment, such as for the study of oriented systems or where

the spectral linewidth is much larger than the attainable MAS frequency. However, significant progress has thus been made to access sample temperatures $\ll 100$ K while also allowing MAS [22], and the results showing improved DNP and increased sensitivity are very promising for this “ultra-low-temperature” regime. Figure 3a shows the effect of decreasing the sample temperature on the ratio of the ^1H ssNMR signals measured in the presence and the absence of μw irradiation suitable for CE DNP, a ratio referred to as $^1\text{H}\epsilon_{\text{on/off}}$, for a model sample doped with a bi-nitroxide polarizing agent. It is clear that as the temperature decreases, $^1\text{H}\epsilon_{\text{on/off}}$ increases. Therefore, the CE DNP mechanism is becoming more efficient at these lower temperatures. However, it is important to highlight that at 55 K $^1\text{H}\epsilon_{\text{on/off}} = 677$, which is a larger value than that given by the ratio of the gyromagnetic ratios of the electron and nucleus, $\gamma_e/\gamma_{\text{H-1}} = 658$, the theoretical maximum nuclear polarization gain in this case. Since nuclei can have an equilibrium polarization that is less than their expected Boltzmann polarization due to depolarization in the presence of the CE but absence of μw irradiation (*vide supra*) then the ratio of equilibrium polarizations of electrons and protons can be > 658 . Therefore, the absolute polarization gain obtained with DNP should be determined using a comparison to the Boltzmann polarization of the nuclei, and $\epsilon_{\text{on/off}}$ does not represent this gain for CE DNP and can thus give misleading values and interpretations.

We introduced the absolute sensitivity ratio (ASR) [23] as a way to encompass all the positive and negative effects that come with performing high-field DNP-enhanced ssNMR experiments and to thus give a good evaluation of the pertinence of performing DNP when compared to conventional ssNMR. Other methods to rationalize this gain have also been proposed [24], and these rely on the multiplication of different contributing factors. The ASR encompasses all of the effects because it is an

experimentally measured value. The sensitivity (signal-to-noise ratio returned per unit square root of time) is compared between spectra from an analyte recorded under DNP conditions and those commonly employed for conventional ssNMR. Therefore, the ASR takes into account such factors as the DNP enhancement, the temperature change (thermal polarization, thermal noise), spin relaxation and coherence lifetimes (temperature and paramagnetic effects), linewidth changes (*vide infra*), usable sample mass (paramagnetic bleaching, sample dilution), and the availability of advanced equipment (larger magnetic fields, smaller/larger MAS rotors). Methods to optimize the ASR, including various ways to prepare samples for DNP experiments, have been discussed elsewhere [24]. Figure 3b shows the effect of decreasing the sample temperature on the ASR of nanotubes of cyclo-diphenylalanine prepared for CE DNP. Already by only using the more customary conditions for DNP-enhanced ssNMR (9 T, 108 K), an ASR of 960 could be obtained. However, by reducing the sample temperature to 50 K, the ASR increased by a factor of 5.6. This means that experiments could be recorded an additional ($5.6^2 =$) 31 times faster. Compared to conventional ssNMR (9 T, 298 K, no paramagnets), an experiment that would have taken 55 years could now be recorded in 1 minute!

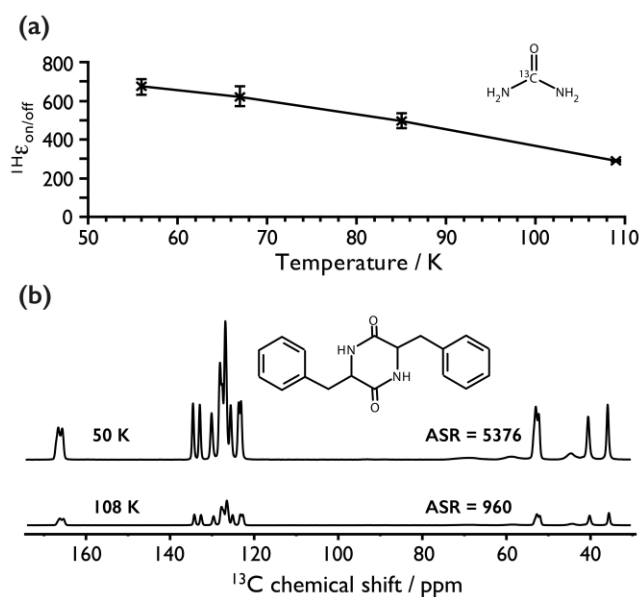


Fig. 3. Analysis of CE DNP with decreasing temperature in a magnetic field of 9 T. (a) The measured DNP-enhancement ratio at a MAS rate of 10 kHz as a function of sample temperature for a ^{13}C -urea (inset) model solution (2M in D_8 -glycerol/ $\text{D}_2\text{O}/\text{H}_2\text{O}$ (6/3/1, v/v/v)) containing 5 mM AMUPol [25] biradical polarizing agent. (b) DNP-enhanced $\{^1\text{H}\}\text{-}^{13}\text{C}$ CP NMR spectra of nanotubes of cyclo-diphenylalanine (inset) containing the AMUPol biradical polarizing agent, recorded at sample temperatures of 108 K (bottom) and 50 K (top) using a MAS rate of 12.5 kHz. The spectra have been scaled relative to their absolute sensitivity. Adapted (combining parts from Figures 3 and 5) with permission from Ref. [26] – Published by The Royal Society of Chemistry.

Biological applications

With the large sensitivity gains that have been shown to be achievable, attention has also been directed at applications of high-field DNP to help study systems of interest. The biological ssNMR community has always strived for better resolution and sensitivity, particularly pushing the development of higher magnetic fields and faster MAS rates. So the successful establishment of high-field ssNMR with DNP was markedly appealing. Since, this technique has been applied to study peptides, proteins, amyloid fibrils, membrane complexes, and even entire intact cells [27]. Unlike solution-state NMR and X-ray crystallography, ssNMR has the potential to study large biomacromolecules that lack long-range order at the atomic scale. Moreover, for those

systems that do exhibit long-range order, it is not always straight-forward to produce sufficient crystals for X-ray analysis, or sometimes these crystals do not represent the molecule's structure in its native biological context. In these cases, ssNMR spectroscopy is then the technique of choice, provided adequate resolution and sensitivity is attainable. Indeed, it has been recently shown that the structure of a particular protein at its natural endogenous concentration in a biological environment (of cell lysates) is different to that of the purified system [28]. This study was only possible with the use of high-field DNP. The intrinsic sensitivity of $\sim 1 \mu\text{M}$ (isotopically-labeled) protein would be too low for the necessary 2D experiments with conventional ssNMR.

To increase resolution for biological studies, which are usually complicated by many overlapping resonances, the highest magnetic fields possible are generally desired. To date, the highest static, continuous field for ssNMR is 24 T, and DNP combined with ssNMR is commercially available up to 19 T. However, the efficiency of the SE and CE DNP mechanisms generally decreases with increasing field strength, with relationships expected to be proportional to B_0^{-2} and B_0^{-1} , respectively. To circumnavigate this *Catch-22* for high-resolution and high-sensitivity biological ssNMR with DNP, further technological and methodological advancements still need to be made; the use of the OE [6] or trityl-nitroxide bi-radicals [29] seem promising. Additionally, DNP enhancements, ${}^1\text{H}_{\epsilon_{\text{on/off}}}$, on *real* systems are usually much inferior to the maximum currently obtained for *model* systems – signal gains depend heavily on the nature of the sample and its preparation – and this is obviously then especially important at 19 T. As such, values at 19 T for ${}^1\text{H}_{\epsilon_{\text{on/off}}}$ of 8 (100 at 9 T) and 15 (60 at 9 T) have been obtained for a membrane-embedded potassium channel protein [30] and a cell-embedded megadalton protein complex [31], respectively; model systems (small

amino acids) prepared in a similar manner would usually return ${}^1\text{H}\epsilon_{\text{on/off}} \sim 35$. The latter study involved probing the large complex in its native environment. This study showed that the 3D fold seen in *in vitro* crystals is also present in the native cellular preparation. For the former experiment on the membrane-embedded potassium channel, the low-temperature conditions and addition of paramagnetic polarizing agent were useful not just for the DNP, which facilitated an ASR of 2.6 (meaning an experiment that would usually take 1 week could be recorded in only 1 day), but they can also provide further information. The exogenous extracellular polarizing agent was used to highlight solvent exposed regions of the protein through paramagnet-induced signal modulations of those regions. Whereas highly dynamic areas of the channel could be detected through increasing linewidths of ${}^{13}\text{C}$ resonances from certain residues at low temperature when compared to ambient temperature measurements.

This increase in linewidth is due to frozen conformational heterogeneity (which is dynamically averaged at ambient temperature) and it puts a limitation on the resolution achievable under current conditions for ssNMR with DNP, since this line broadening is proportional to the magnetic field. Figure 4a compares 2D ${}^{13}\text{C}$ - ${}^{13}\text{C}$ proton-driven spin diffusion (PDS) spectra recorded on the potassium channel with DNP at 9 and 19 T [30]. It is clear that the resolution of some ${}^{13}\text{C}$ cross peaks has improved, whereas for others it has stayed the same. Furthermore, Figure 4b compares the same data from Figure 4a recorded at 19 T with DNP with a corresponding 16 T ssNMR spectrum, recorded under conventional ambient temperature conditions. It is clear from Figures 4a and 4b that there are two types of dominant broadening present, homogeneous and inhomogeneous. For those peaks that are homogeneously broadened, an increase in magnetic field strength can make an important contribution to spectral resolution. However, as particularly demonstrated in Figure 4b, when there is

significant inhomogeneous broadening at low temperatures it can severely impede spectral resolution. Moreover, for ^{15}N , which is also extensively probed for studies of biomolecules, it is known and also shown [32] that it is even more sensitive to conformational disorder than ^{13}C . Accordingly, this can result in substantial inhomogeneous broadening for ^{15}N NMR under DNP conditions at 9 and 14 T [32], as well as at 19 T [30].

One way to lessen resolution issues is specific isotopic labeling, as this will decrease the number of overlapping resonances and, as such, this has been comprehensively employed for conventional NMR of biomolecules. Combining labeling schemes with DNP can therefore be pivotal and has been used, for instance, to investigate the interface, and thus interactions, between proteins in oligomeric complexes within a lipid bilayer [33]. This interface is relatively small and thus would normally be undetectable without the sensitivity gains afforded by DNP. Specific isotopic replacement of ^1H with ^2H has also been used. Although reducing the ^1H concentration may reduce the efficiency of ^1H - ^1H spin-diffusion to distribute the hyperpolarization to all the ^1H in the system, it has been shown that it can improve CE DNP, leading to larger $^{1\text{H}}\epsilon_{\text{on/off}}$ for biomolecules [32, 34]. However, the reduced ^1H content can also impact the efficacy of CP, meaning that there may actually be no overall net gain in sensitivity (ASR) [32].

It is interesting to note that studies of biomolecules can be made using high-field ssNMR with OE DNP at ambient temperature, thereby maintaining molecular mobility [35]. This premise shows much potential. However, it has only so far been demonstrated with singly-tunable radio-frequency NMR circuits, with restricted amounts of (static) sample, and at magnetic fields strengths of 9 T. Large technical advances are required to make this interesting approach widely applicable.

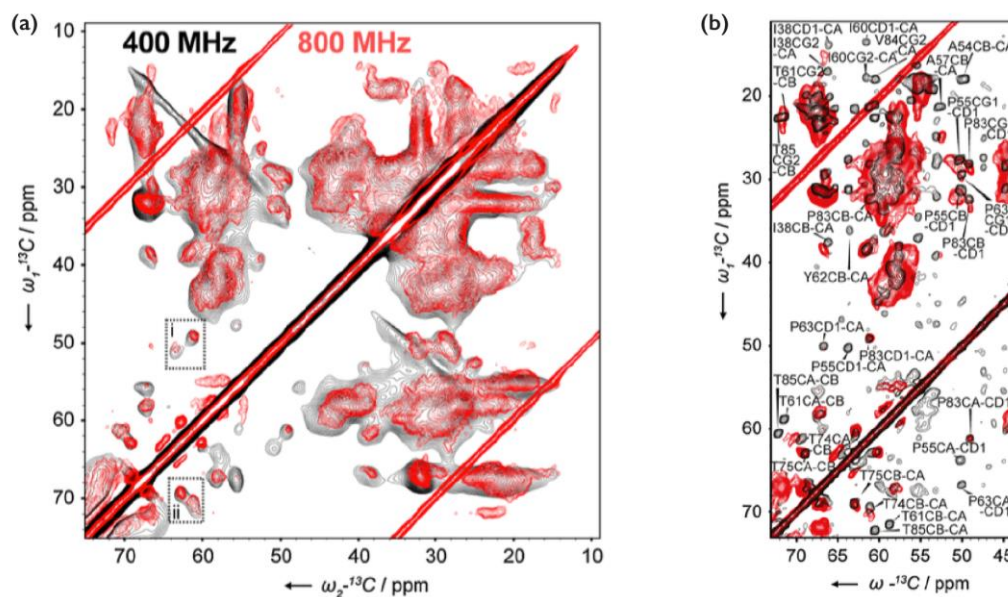


Fig. 4. (a) DNP-enhanced ^{13}C - ^{13}C PSD correlation spectra of a membrane-embedded potassium channel protein, recorded in magnetic fields of 9 T (black) and 19 T (red). (b) The same DNP-enhanced spectrum recorded at 19 T from (a, red) compared to a corresponding conventional ambient temperature ssNMR spectrum recorded at 16 T (black). Adapted with permission from Ref. [30].

Along with the intricate study of biomolecules, DNP is creating pathways to advanced atomic-level characterization of other biological systems, such as biominerals like hydroxyapatite [36]. Hydroxyapatite has calcium as a main constituent (as well as P, O, and H), but the NMR-active isotope of calcium, ^{43}Ca , is an exceptionally insensitive nucleus (spin-7/2, $|\gamma_{\text{Ca-43}}|/\gamma_{\text{H-1}} \sim 0.07$), made much worse by its extremely low natural isotopic abundance (0.14%). Therefore, there are few ^{43}Ca ssNMR studies, and obviously even fewer using ^{43}Ca at natural abundance (NA). Despite these limitations, it has been recently shown that DNP can be used to greatly facilitate high-field ^{43}Ca ssNMR spectroscopy [36]. Figure 5a compares a ^{43}Ca spectrum acquired in < 1 hour on hydroxyapatite at 9 T with the use of DNP and a corresponding spectrum recorded with the benefit of low temperatures (100 K) and double-frequency sweep preparation in > 5 hours. It is clear that the sensitivity of the experiment recorded with DNP is

orders of magnitude greater. Indeed, the ASR for this study was at least 35. The sensitivity was such that 2D spectra could be recorded, which allowed the elucidation of surface and bulk ^{43}Ca sites (see Figure 5b). The unprecedented sensitivity then suggests that a fuller atomic-level analysis of biominerals can be completed, through the observation of (usually) insensitive nuclei and/or nuclei at low weight % in the system, such as ^{13}C in carbonated hydroxyapatite [36]. Moreover, many biomolecules also contain metal nuclei, such as ^{25}Mg , ^{43}Ca , and ^{67}Zn , which are crucial to their structure and function but are at low weight % and also usually extremely insensitive, and they are consequently very difficult to detect directly. DNP may then enable ssNMR to access their local environment, providing a key understanding of their biological function and properties.

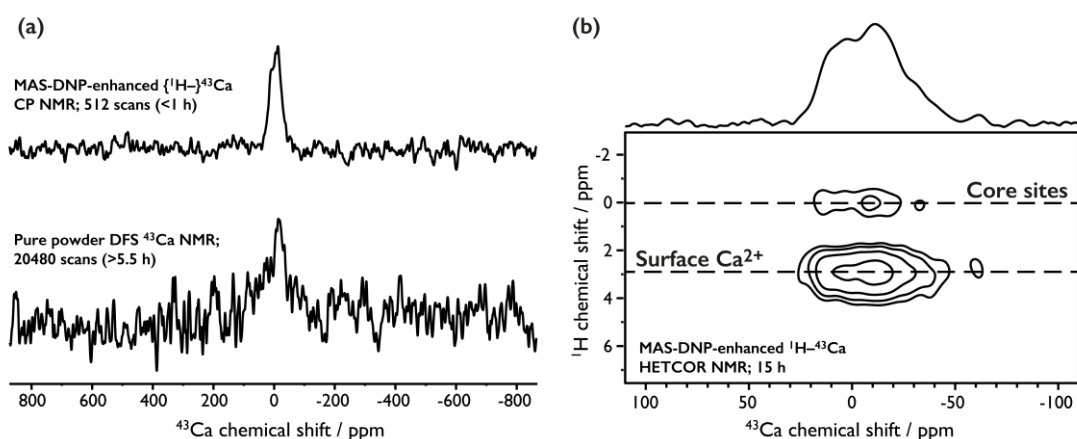


Fig. 5. DNP-enhanced 1D (a, top) and 2D (b) ^1H - ^{43}Ca CP spectra of carbonated nanoparticulate hydroxyapatite, recorded at natural isotopic abundance in a magnetic field of 9 T. Adapted (combining parts from Figures 3 and 4) with permission from Ref [36].

Chemical applications

Applications of high-field ssNMR with DNP to materials ranging from organic to inorganic, with hybrids in between, have been plentiful in recent years [24], with

particular interest paid to surfaces [37]. Unlike biomolecules, isotopic labeling of (non-bio)materials can be challenging or expensive (or both). Therefore, working at NA, if possible, can be highly advantageous. This was shown (*vide supra*) to be now possible for ^{43}Ca (NA = 0.14 %) with the sensitivity gain provided by CE DNP. Furthermore, high-field CE DNP has already made NA ssNMR of ^{15}N (NA = 0.37 %) [38], ^{17}O (NA = 0.04 %) [39], as well as ^2H (NA = 0.01 %) [40] readily accessible.

^{15}N ssNMR should be particularly important for small organic-based materials, which have an almost boundless variety of uses, ranging from medicine to electronics. Nitrogen is ubiquitous in these systems, it is often involved in structural interactions (such as hydrogen bonding), and ^{15}N can provide highly resolved resonances with a wide chemical shift dispersion. ^{15}N should therefore be a quintessential NMR target for the detailed study of these types of systems. However, its low NMR sensitivity (NA = 0.37 %, $|\gamma_{\text{N-15}}/\gamma_{\text{H-1}}| \sim 0.1$) prohibits its extensive exploitation when isotopic labeling is difficult. Consequently, high-field DNP has provided a major breakthrough in this area by producing sufficient NMR sensitivity to readily record experiments involving ^{15}N at NA. Recently, DNP was used to obtain this type of data for pharmaceutical formulations [41]. Figure 6 shows DNP-enhanced NMR data from crystalline cetirizine dihydrochloride, an active pharmaceutical ingredient (API), at NA. The substantial increase in NMR sensitivity supplied by the DNP permitted the fast acquisition of ^{13}C (NA = 1.1 %) homonuclear correlation data (Figure 6a), allowing the assignment of the ^{13}C resonances from the API. Moreover, $\{^1\text{H}\}\text{-}^{15}\text{N}$ CP spectra (Figure 6b) and 2D $^1\text{H}\text{-}^{15}\text{N}$ dipolar correlation spectra could be recorded, not only for the pure API but also for the API in its pharmaceutical formulation, which contains diluting excipients. This enabled the comparison of formulations (from different commercial retailers), highlighting that it was the amorphous form of the API that was present in each, and

also notably that surface molecules from the sub- μm domains of the amorphous API interact with an excipient. This latter conclusion, drawn from ^1H - ^{15}N dipolar interactions (and not observed through corresponding ^1H - ^{13}C dipolar correlation spectra), is extremely important because these interactions can determine the rate at which the API is released from the formulation.

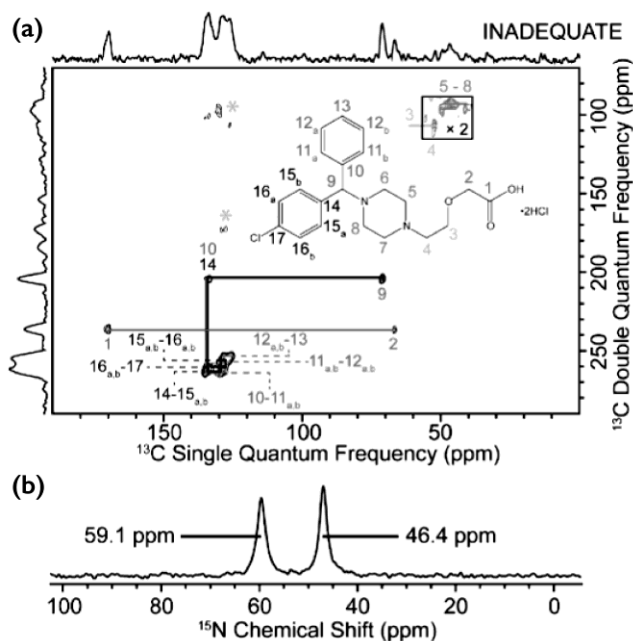


Fig. 6. DNP-enhanced ^{13}C - ^{13}C correlation spectrum (a) and $\{^1\text{H}\}$ - ^{15}N CP spectrum (b) of crystalline cetirizine dihydrochloride (inset in (a)), recorded at natural isotopic abundance in a magnetic field of 9 T. Adapted from Ref. [41]. Copyright 2014 American Chemical Society.

Further work employing DNP for the study of organic materials has also exploited 2D experiments involving ^{15}N . Figure 7 illustrates correlation data from such an experiment, whereby ^{13}C and ^{15}N through-space proximities were probed at NA (1.1 % and 0.37 %, respectively – leading to a spin-pair probability of 0.004 % compared to a fully enriched sample) [42]. These correlations were used to complete a *de novo* resonance assignment for the two molecules in the asymmetric crystallographic unit cell of the studied system, a ribbon-forming guanosine-based architecture (2'-deoxy-

3',5'-dipropanoylguanosine). Along with work momentarily expedited by the use of high-field DNP for the study of NA ^{13}C - ^{13}C connectivities with ssNMR [23], the ^{13}C - ^{15}N work paves the way to the fast *de novo* elucidation of structures of organic materials using NA samples.

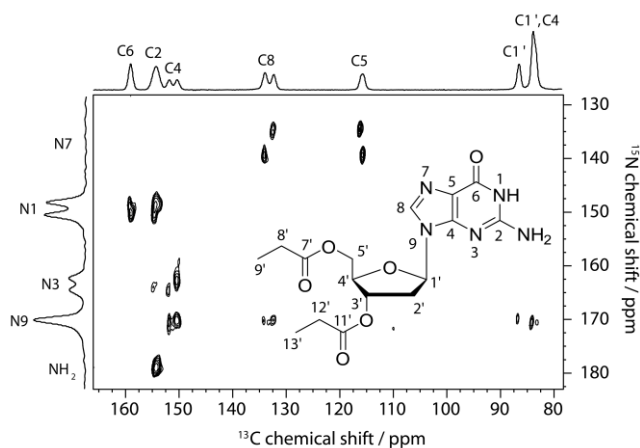


Fig. 7. DNP-enhanced ^{13}C - ^{15}N correlation spectrum of a guanosine-based system (inset) that can self-assemble into a ribbon-like nanomaterial, recorded at natural isotopic abundance in a magnetic field of 9 T. Adapted from Ref. [42]. Copyright 2015 American Chemical Society.

The sensitivity gain provided by high-field DNP has also allowed the measurement of internuclear distances for spins with low NA in an important class of inorganic materials, namely solid oxides [43, 44]. The surface and/or the bulk of these materials can be crucial to their function, and thus application, so a thorough understanding of both is highly desired (and as such has been studied using high-field DNP [45, 46]). ^{29}Si - ^{29}Si distances (as well as $^2J^{\text{Si-O-Si}}$ -couplings) could be measured for NA surface nuclei of functionalized silica (SiO_2) nanoparticles owing to the sensitivity gains resulting from the successful implementation of high-field DNP for ssNMR experiments ($\text{ASR} = 25$) [43]. Moreover, the covalent structure of the functionalizing organic molecules in this hybrid system could be obtained through

homonuclear correlation experiments, which showed that the preferred lateral surface functionalization was indeed present, providing the maximum surface area for the functional molecules. In addition to silica nanoparticles, porous silicas are also indispensable due to their high area surfaces that can be easily functionalized. Functionalization usually begins with the surface silanol (SiOH) groups, so knowledge of their hydrogen bonding and dynamics could be decisive in the functionalization process(es). To this extent it was shown that these silanol groups could be probed through NA 2D ^1H - ^{17}O correlation ssNMR experiments, again thanks to the increases in sensitivity bestowed by DNP [44]. This is no mean feat since the only stable NMR-active isotope of oxygen, ^{17}O , is a spin-5/2 nucleus with a moderately low gyromagnetic ratio ($|\gamma_{\text{O-17}}/\gamma_{\text{H-1}}| \sim 0.1$) and an especially low NA (0.04 %). Nevertheless, with DNP, ^1H - ^{17}O distances could be extracted, along with a quantitative analysis of librational motions of the corresponding silanols. Moreover, as shown in Figure 8, a change in the hydrogen-bonded and lone silanols upon pre-heating *in vacuo* could be followed with ^{17}O NMR, based on the 2D data.

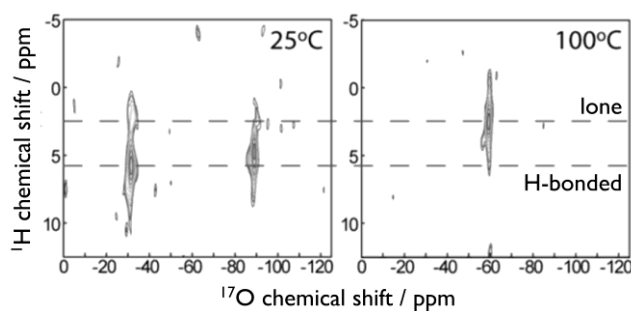


Fig. 8. DNP-enhanced ^1H - ^{17}O correlation spectra of mesoporous silica nanoparticles pre-treated *in vacuo* at different temperatures, recorded at natural isotopic abundance in a magnetic field of 9 T, highlighting lone and hydrogen-bonded silanols (dashed lines). Adapted from Ref. [44]. Copyright 2016 American Chemical Society.

Along with the examples of ^{43}Ca and ^{17}O , high-field DNP has provided access to fast ssNMR studies of other quadrupolar nuclei, such as ^{35}Cl [20], ^{27}Al [47, 48], and ^{14}N [49]. It has thus opened the flood gates to a whole range of studies that were previously inaccessible. This is especially important because quadrupolar nuclei account for $> 3/4$ of all NMR-active isotopes and are present in most materials. Taking the technique further still, as for the case of biomolecules, will require efficient DNP at even higher fields. Here, studies of quadrupolar nuclei could benefit greatly since their observed ssNMR linewidth, when dominated by their quadrupolar interaction (as is usually the case), is inversely proportional to the field strength. However, as stated above, there is still much work to be done to realise efficient DNP at ≥ 19 T.

Conclusions and Outlook

There is a current revolution in solid-state NMR and it owes a lot to the commercialization of an experimental setup that provides low temperature MAS NMR along with suitable continuous microwave irradiation of the sample, which followed on from the groundbreaking work of Griffin and co-workers. The experimental setup is under constant development, with access to lower sample temperatures using cold helium gas in combination with MAS and opportunities arising from alternative microwave sources such as those that are pulse, phase, and frequency adjustable, providing large interest. Furthermore, the introduction of NMR probes capable of rapid sample spinning using smaller diameter rotors (currently down to 1.3 mm) at low temperatures advances the use of higher-field DNP (currently up to 19 T) [50] and also permits experiments in a new regime.

It has been demonstrated herein that there has been much progress in high-field ssNMR with DNP, which has resulted in great sensitivity gains. These have not just facilitated, but in numerous cases enabled, intricate experiments on a variety of systems ranging from biomolecules to inorganic-organic hybrid nanomaterials. For biomolecular studies DNP has, for example, permitted the comparison of a protein in its natural biological context and as a purified system, showing that the structure differed depending on the environment. For inorganic-organic hybrid nanomaterials DNP has allowed, for example, studies of the surface grafting of functionalizing moieties, showing that lateral and vertical functionalization could be differentiated.

Although high-field ssNMR with DNP is fast becoming a routine atomic-level characterization tool, substantial advancements can still be made. Spectral resolution, sample preparation, ultra-fast MAS, and sensitivity could all still benefit further from methodological and technological improvements. Therefore, this technique, which is already showing broad and potent employment, can only become more useful, ubiquitous, and influential.

References

1. Overhauser, A.: Polarization of Nuclei in Metals. *Phys. Rev.* 92, 411–415 (1953).
2. Carver, T.R., Slichter, C.P.: Polarization of Nuclear Spins in Metals. *Phys. Rev.* 92, 212–213 (1953).
3. Wind, R.A.: Dynamic Nuclear Polarization and High-Resolution NMR of

- Solids. In: Harris, R.K. and Wasylshen, R.L. (eds.) *Encyclopedia of Magnetic Resonance*. pp. 1–10. John Wiley & Sons, Ltd, Chichester, UK (2007).
4. Hall, D.A., Maus, D.C., Gerfen, G.J., Inati, S.J., Becerra, L.R., Dahlquist, F.W., Griffin, R.G.: Polarization-Enhanced NMR Spectroscopy of Biomolecules in Frozen Solution. *Science* (80-.). 276, 930–932 (1997).
 5. Can, T.V., Ni, Q.Z., Griffin, R.G.: Mechanisms of dynamic nuclear polarization in insulating solids. *J. Magn. Reson.* 253, 23–35 (2015).
 6. Can, T. V, Caporini, M.A., Mentink-Vigier, F., Corzilius, B., Walish, J.J., Rosay, M., Maas, W.E., Baldus, M., Vega, S., Swager, T.M., Griffin, R.G.: Overhauser effects in insulating solids. *J. Chem. Phys.* 141, 64202 (2014).
 7. Mentink-Vigier, F., Akbey, Ü., Hovav, Y., Vega, S., Oschkinat, H., Feintuch, A.: Fast passage dynamic nuclear polarization on rotating solids. *J. Magn. Reson.* 224, 13–21 (2012).
 8. Thurber, K.R., Tycko, R.: Theory for cross effect dynamic nuclear polarization under magic-angle spinning in solid state nuclear magnetic resonance: the importance of level crossings. *J. Chem. Phys.* 137, 84508 (2012).
 9. Thurber, K.R., Tycko, R.: Perturbation of nuclear spin polarizations in solid state NMR of nitroxide-doped samples by magic-angle spinning without microwaves. *J. Chem. Phys.* 140, 184201 (2014).
 10. Mentink-Vigier, F., Paul, S., Lee, D., Feintuch, A., Hediger, S., Vega, S., De Paëpe, G.: Nuclear Depolarization and Absolute Sensitivity in Magic Angle Spinning Cross Effect Dynamic Nuclear Polarization. *Phys. Chem. Chem. Phys.*

Accepted (2015).

11. Mentink-Vigier, F., Vega, S., De Paëpe, G.: Large spin ensembles for MAS-DNP. *Phys. Chem. Chem. Phys.* (2016).
12. Hu, K.-N., Yu, H., Swager, T.M., Griffin, R.G.: Dynamic nuclear polarization with biradicals. *J. Am. Chem. Soc.* 126, 10844–10845 (2004).
13. Sauvée, C., Casano, G., Abel, S., Rockenbauer, A., Akhmetzyanov, D., Karoui, H., Siri, D., Aussenac, F., Maas, W., Weber, R.T., Prisner, T., Rosay, M., Tordo, P., Ouari, O.: Tailoring of Polarizing Agents in the bTurea Series for Cross-Effect Dynamic Nuclear Polarization in Aqueous Media. *Chem. - A Eur. J.* 22, 5598–5606 (2016).
14. Vitzthum, V., Borcard, F., Jannin, S., Morin, M., Mieville, P., Caporini, M.A., Sienkiewicz, A., Gerber-Lemaire, S., Bodenhausen, G.: Fractional spin-labeling of polymers for enhancing NMR sensitivity by solvent-free dynamic nuclear polarization. *Chemphyschem.* 12, 2929–2932 (2011).
15. Fernández-de-Alba, C., Takahashi, H., Richard, A., Chenavier, Y., Dubois, L., Maurel, V., Lee, D., Hediger, S., De Paëpe, G.: Matrix-Free DNP-Enhanced NMR Spectroscopy of Liposomes Using a Lipid-Anchored Biradical. *Chem. - A Eur. J.* 21, 4512–4517 (2015).
16. Maly, T., Cui, D., Griffin, R.G., Miller, A.-F.: ¹H dynamic nuclear polarization based on an endogenous radical. *J. Phys. Chem. B.* 116, 7055–7065 (2012).
17. Riikonen, J., Rigolet, S., Marichal, C., Aussenac, F., Lalevée, J., Morlet-Savary, F., Fioux, P., Dietlin, C., Bonne, M., Lebeau, B., Lehto, V.-P.: Endogenous

- Stable Radicals for Characterization of Thermally Carbonized Porous Silicon by Solid-State Dynamic Nuclear Polarization ^{13}C NMR. *J. Phys. Chem. C*. 119, 19272–19278 (2015).
18. Armstrong, B.D., Edwards, D.T., Wylde, R.J., Walker, S.A., Han, S.: A 200 GHz dynamic nuclear polarization spectrometer. *Phys. Chem. Chem. Phys.* 12, 5920–5926 (2010).
 19. Salnikov, E.S., Aisenbrey, C., Aussenac, F., Ouari, O., Sarrouj, H., Reiter, C., Tordo, P., Engelke, F., Bechinger, B.: Membrane topologies of the PGLa antimicrobial peptide and a transmembrane anchor sequence by Dynamic Nuclear Polarization/solid-state NMR spectroscopy. *Sci. Rep.* 6, 20895 (2016).
 20. Hirsh, D.A., Rossini, A.J., Emsley, L., Schurko, R.W.: ^{35}Cl Dynamic Nuclear Polarization Solid-State NMR of Active Pharmaceutical Ingredients. *Phys. Chem. Chem. Phys.* (2016).
 21. Kobayashi, T., Perras, F.A., Goh, T.W., Metz, T.L., Huang, W., Pruski, M.: DNP-Enhanced Ultrawideline Solid-State NMR Spectroscopy: Studies of Platinum in Metal–Organic Frameworks. *J. Phys. Chem. Lett.* 7, 2322–2327 (2016).
 22. Lee, D., Bouleau, E., Saint-Bonnet, P., Hediger, S., De Paëpe, G.: Ultra-low temperature MAS-DNP. *J. Magn. Reson.* 264, 116–124 (2016).
 23. Takahashi, H., Lee, D., Dubois, L., Bardet, M., Hediger, S., De Paëpe, G.: Rapid natural-abundance 2D ^{13}C - ^{13}C correlation spectroscopy using dynamic nuclear polarization enhanced solid-state NMR and matrix-free sample preparation. *Angew. Chem. Int. Ed. Engl.* 51, 11766–9 (2012).

24. Lee, D., Hediger, S., De Paëpe, G.: Is solid-state NMR enhanced by dynamic nuclear polarization? *Solid State Nucl. Magn. Reson.* 66–67, 6–20 (2015).
25. Sauvée, C., Rosay, M., Casano, G., Aussenac, F., Weber, R.T., Ouari, O., Tordo, P.: Highly Efficient, Water-Soluble Polarizing Agents for Dynamic Nuclear Polarization at High Frequency. *Angew. Chemie Int. Ed.* 52, 10858–10861 (2013).
26. Bouleau, E., Saint-Bonnet, P., Mentink-Vigier, F., Takahashi, H., Jacquot, J.-F., Bardet, M., Aussenac, F., Porea, A., Engelke, F., Hediger, S., Lee, D., De Paëpe, G.: Pushing NMR sensitivity limits using dynamic nuclear polarization with closed-loop cryogenic helium sample spinning. *Chem. Sci.* 6, 6806–6812 (2015).
27. Su, Y., Andreas, L., Griffin, R.G.: Magic Angle Spinning NMR of Proteins: High-Frequency Dynamic Nuclear Polarization and ^1H Detection. *Annu. Rev. Biochem.* 84, 465–497 (2015).
28. Frederick, K.K., Michaelis, V.K., Corzilius, B., Ong, T.-C., Jacavone, A.C., Griffin, R.G., Lindquist, S.: Sensitivity-Enhanced NMR Reveals Alterations in Protein Structure by Cellular Milieus. *Cell.* 163, 620–628 (2015).
29. Mathies, G., Caporini, M.A., Michaelis, V.K., Liu, Y., Hu, K.-N., Mance, D., Zweier, J.L., Rosay, M., Baldus, M., Griffin, R.G.: Efficient Dynamic Nuclear Polarization at 800 MHz/527 GHz with Trityl-Nitroxide Biradicals. *Angew. Chemie Int. Ed.* n/a-n/a (2015).
30. Koers, E.J., van der Crujisen, E.A.W., Rosay, M., Weingarth, M., Prokofyev, A., Sauvée, C., Ouari, O., van der Zwan, J., Pongs, O., Tordo, P., Maas, W.E.,

- Baldus, M.: NMR-based structural biology enhanced by dynamic nuclear polarization at high magnetic field. *J. Biomol. NMR.* 60, 157–168 (2014).
31. Kaplan, M., Cukkemane, A., van Zundert, G.C.P., Narasimhan, S., Daniëls, M., Mance, D., Waksman, G., Bonvin, A.M.J.J., Fronzes, R., Folkers, G.E., Baldus, M.: Probing a cell-embedded megadalton protein complex by DNP-supported solid-state NMR. *Nat. Methods.* 12, 649–652 (2015).
 32. Liao, S.Y., Lee, M., Wang, T., Sergeyev, I. V., Hong, M.: Efficient DNP NMR of membrane proteins: sample preparation protocols, sensitivity, and radical location. *J. Biomol. NMR.* 64, 223–237 (2016).
 33. Maciejko, J., Mehler, M., Kaur, J., Lieblein, T., Morgner, N., Ouari, O., Tordo, P., Becker-Baldus, J., Glaubitz, C.: Visualizing Specific Cross-Protomer Interactions in the Homo-Oligomeric Membrane Protein Proteorhodopsin by Dynamic-Nuclear-Polarization-Enhanced Solid-State NMR. *J. Am. Chem. Soc.* 137, 9032–9043 (2015).
 34. Akbey, Ü., Franks, W.T., Linden, A.H., Lange, S., Griffin, R.G., van Rossum, B.-J., Oschkinat, H.: Dynamic nuclear polarization of deuterated proteins. *Angew. Chem. Int. Ed. Engl.* 49, 7803–7806 (2010).
 35. Jakdetchai, O., Denysenkov, V., Becker-Baldus, J., Dutagaci, B., Prisner, T.F., Glaubitz, C.: Dynamic Nuclear Polarization-Enhanced NMR on Aligned Lipid Bilayers at Ambient Temperature. *J. Am. Chem. Soc.* 136, 15533–15536 (2014).
 36. Lee, D., Leroy, C., Crevant, C., Bonhomme-Coury, L., Babonneau, F., Laurencin, D., Bonhomme, C., De Paëpe, G.: Interfacial Ca²⁺ environments in nanocrystalline apatites revealed by dynamic nuclear polarization enhanced

- ⁴³Ca NMR spectroscopy. *Nat. Commun.* (2016).
37. Rossini, A.J., Zagdoun, A., Lelli, M., Lesage, A., Copéret, C., Emsley, L.: Dynamic nuclear polarization surface enhanced NMR spectroscopy. *Acc. Chem. Res.* 46, 1942–1951 (2013).
 38. Rossini, A.J., Zagdoun, A., Lelli, M., Canivet, J., Aguado, S., Ouari, O., Tordo, P., Rosay, M., Maas, W.E., Copéret, C., Farrusseng, D., Emsley, L., Lesage, A.: Dynamic nuclear polarization enhanced solid-state NMR spectroscopy of functionalized metal-organic frameworks. *Angew. Chemie (International Ed.* 51, 123–127 (2012).
 39. Blanc, F., Sperrin, L., Jefferson, D.A., Pawsey, S., Rosay, M., Grey, C.P.: Dynamic nuclear polarization enhanced natural abundance ¹⁷O spectroscopy. *J. Am. Chem. Soc.* 135, 2975–2978 (2013).
 40. Rossini, A.J., Schlagnitweit, J., Lesage, A., Emsley, L.: High-resolution NMR of hydrogen in organic solids by DNP enhanced natural abundance deuterium spectroscopy. *J. Magn. Reson.* 259, 192–198 (2015).
 41. Rossini, A.J., Widdifield, C.M., Zagdoun, A., Lelli, M., Schwarzwälder, M., Coperet, C., Lesage, A., Emsley, L.: DNP Enhanced NMR Spectroscopy for Pharmaceutical Formulations. *J. Am. Chem. Soc.* 140110190741000 (2014).
 42. Märker, K., Pingret, M., Mouesca, J.-M., Gasparutto, D., Hediger, S., De Paëpe, G.: A New Tool for NMR Crystallography: Complete ¹³C/ ¹⁵N Assignment of Organic Molecules at Natural Isotopic Abundance Using DNP-Enhanced Solid-State NMR. *J. Am. Chem. Soc.* 137, 13796–13799 (2015).

43. Lee, D., Monin, G., Duong, N.T., Zamanillo Lopez, I., Bardet, M., Mareau, V., Gonon, L., De Paëpe, G.: Untangling the Condensation Network of Organosiloxanes on Nanoparticles using 2D ^{29}Si - ^{29}Si Solid-State NMR enhanced by Dynamic Nuclear Polarization. *J. Am. Chem. Soc.* 136, 13781–13788 (2014).
44. Perras, F.A., Chaudhary, U., Slowing, I.I., Pruski, M.: Probing Surface Hydrogen Bonding and Dynamics by Natural Abundance, Multidimensional, ^{17}O DNP-NMR Spectroscopy. *J. Phys. Chem. C.* 120, 11535–11544 (2016).
45. Lafon, O., Rosay, M., Aussenac, F., Lu, X., Trébosc, J., Cristini, O., Kinowski, C., Touati, N., Vezin, H., Amoureux, J.-P.: Beyond the silica surface by direct silicon-29 dynamic nuclear polarization. *Angew. Chemie (International Ed.)* 50, 8367–8370 (2011).
46. Lee, D., Duong, N.T., Lafon, O., De Paëpe, G.: Primostrato Solid-state Nmr Enhanced by Dynamic Nuclear Polarization: Penta-coordinated Al are Only Located at the Surface of Hydrated γ -alumina. *J. Phys. Chem. C.* 118, 25065–25076 (2014).
47. Vitzthum, V., Miéville, P., Carnevale, D., Caporini, M. a, Gajan, D., Copéret, C., Lelli, M., Zagdoun, A., Rossini, A.J., Lesage, A., Emsley, L., Bodenhausen, G.: Dynamic nuclear polarization of quadrupolar nuclei using cross polarization from protons: surface-enhanced aluminium-27 NMR. *Chem. Commun. (Camb.)* 48, 1988–1990 (2012).
48. Lee, D., Takahashi, H., Thankamony, A.S.L., Dacquin, J.-P., Bardet, M., Lafon, O., Paëpe, G. De: Enhanced solid-state NMR correlation spectroscopy of

- quadrupolar nuclei using dynamic nuclear polarization. *J. Am. Chem. Soc.* 134, 18491–4 (2012).
49. Rossini, A.J., Emsley, L., O'Dell, L.A.: Dynamic nuclear polarisation enhanced ¹⁴N overtone MAS NMR spectroscopy. *Phys. Chem. Chem. Phys.* 16, 12890–12899 (2014).
50. Chaudhari, S.R., Berruyer, P., Gajan, D., Reiter, C., Engelke, F., Silverio, D.L., Copéret, C., Lelli, M., Lesage, A., Emsley, L.: Dynamic nuclear polarization at 40 kHz magic angle spinning. *Phys. Chem. Chem. Phys.* 18, 10616–10622 (2016).